PERGAMON

International Journal of Multiphase Flow 27 (2001) 1065–1077

International Journal of Multiphase Flow

www.elsevier.com/locate/ijmulflow

Spectral characteristics of eddy interaction models

David I. Graham *

Department of Mathematics and Statistics, University of Plymouth, Drake Circus, Devon, Plymouth PL4 8AA, UK

Received 4 November 1999; received in revised form 5 October 2000

Abstract

The eddy interaction model (EIM) is in common use in simulations of turbulent particulate flow. In the model, particle motions are determined by interactions with random-velocity fluid eddies. Spatial and temporal velocity autocorrelations (and therefore wave number and frequency spectra) are characterised by the probability distributions of the velocity, length and time scales of the eddies. In this paper, spectral behaviour of both standard and modified EIMs is examined. The whole range of behaviours of the EIM, characterised by polynomial velocity autocorrelation functions, is studied. It is shown that each of the resulting spectra exhibits unphysical characteristics. Consequences for modelling are discussed briefly.

1. Introduction

The energy spectrum is described in Batchelor (1953, p. 36) as 'the single most important quantity in the problem' (of homogeneous turbulence). These spectra decompose the turbulence kinetic energy of the flow into contributions from different wavelengths. The spectrum at a given wavelength measures the mean energy associated with that wavelength. Many important features have been isolated using spectral analysis. A spectral analysis can be used to investigate the exchange of energy from one component to another. It is well known that the production of turbulence occurs at large scales, with viscous dissipation at small length scales. Between these frequencies occurs the familiar cascade of energy from large to small scale motions (see Tennekes and Lumley, 1972). Kolmogorov (1941, cited in Batchelor, 1953) postulated the existence of an inertial range where the spectra are expected to be unaffected by details of production or dissipation. Because of the lack of influence of production or dissipation, the energy spectra in the

* Tel.: +44-1752-232-746; fax: +44-1752-232-780.
E-mail address: dgraham@plymouth.ac.uk (D.I. Graham).

0301-9322/01/$ - see front matter
PII: S0301-9322(00)00062-8

inertial range occurs universally. The energy spectrum in the inertial range is proportional to $k^{-5/3}$.

As well as being important in the study of single-phase turbulence, spectral analysis is commonly used in studies of multiphase flows. Snyder and Lumley (1971) and Wells and Stock (1983) used a spectral analysis to confirm the self-preserving nature of a particle-laden decaying grid turbulence. In further experiments on grid turbulence in water and air, respectively, Schreck and Kleis (1993) and Hussainov et al. (1999) showed an increase in the energy spectrum at high wave numbers. In a study of bubbly air–water flow, Lance and Bataille (1991) observed a much larger increase in spectra at high wave number, an effect ascribed to wake-shedding from the bubbles. On the other hand, frequency (rather than wave number) spectra from experiments carried out by Hetsroni and Sokolov in 1971 (cited in Hetsroni, 1989) in a particle-laden jet flow indicated a decrease in energy at high frequencies.

Numerical studies have also attempted to investigate spectral behaviour in multiphase flows. Generally, direct numerical simulation (DNS) methods have been used. Squires and Eaton (1990, 1991) showed changes in energy spectra due to particles in a forced isotropic turbulence. The spectra were used to show that the DNS simulations included adequate resolution of fluid motions at all scales. It was also clear that the spectra were completely isotropic at all scales. Elghobashi and Truesdell (1993) DNS of decaying isotropic turbulence confirmed that most of the energy in a forced isotropic turbulence was associated with low-frequency motions. They also noted the tendency for particles to decrease the energy at low wave numbers, with a corresponding increase at high wave numbers, leading to the existence of a spectral pivot, a phenomenon which was also confirmed by Boivin et al. (1999) and Sundaram and Collins (1999) in forced and decaying isotropic turbulence, respectively.

It is clear from the discussion above that energy spectra can provide useful information and lead to greater understanding of turbulent multiphase flows. Much information can be obtained from DNS simulations of such flows. It is therefore of interest to reflect upon the spectral behaviour seen in numerical multiphase flow models less sophisticated than DNS. DNS methods are examples of Lagrangian models in which characteristics of a dispersed phase transported by a turbulent carrier flow are found by tracking individual particles. DNS is the most sophisticated of a number of different Lagrangian models (see Graham (1998b) for a discussion on other models). In the following, we look at the spectral characteristics of the simplest Lagrangian multiphase flow model – the eddy interaction model (EIM) first introduced by Gosman and Ioannides (1981). More general conclusions regarding related Lagrangian models will eventually be drawn.

1.1. Energy and dissipation spectra

Energy (wave number) spectra in homogeneous, isotropic turbulence are dependent on the longitudinal and lateral autocorrelations $f(r)$ and $g(r)$, defined by

$$\begin{aligned} f(r) &= R_{11}(r,0,0) = \langle u_1'(0,0,0)u_1'(r,0,0)\rangle, \\ g(r) &= R_{22}(r,0,0) = R_{33}(r,0,0) = \langle u_3'(0,0,0)u_3'(r,0,0)\rangle, \end{aligned} \tag{1}$$

where $u_i(x_1,x_2,x_3)$ is the velocity vector at point (x_1,x_2,x_3) in the flow and the dashes refer to fluctuating parts.

The energy spectrum is then given by (Batchelor, 1953)

$$E(k) = \frac{k}{\pi} \int_0^\infty [f(r) + 2g(r)] \sin(kr) r \, \mathrm{d}r. \tag{2}$$

Assuming incompressibility of the turbulence, the von Karman relation

$$g(r) = f(r) + rf'(r)/2 \tag{3}$$

can be used. The expression for the energy spectrum then becomes

$$E_{\mathrm{vK-H}}(k) = \frac{k}{\pi} \int_0^\infty [3f(r) + rf'(r)] \sin(kr) r \, \mathrm{d}r. \tag{4}$$

However, we note here that EIMs do not enforce the incompressibility condition so that von Karman–Howarth is no longer valid and the correct expression for the energy spectrum is Eq. (2) and NOT Eq. (4).

Corresponding to each energy spectrum is a dissipation spectrum defined by

$$D(k) = 2\pi k^2 E(k). \tag{5}$$

Without loss of generality, we assume in the following analysis that (i) the integral length scale is 1; (ii) the turbulence intensity is 1. In this case, the total energy is

$$\int_0^\infty E(k) \, \mathrm{d}k = 3/2. \tag{6}$$

The total dissipation is given as the integral of the dissipation spectrum:

$$\varepsilon = \int_0^\infty D(k) \, \mathrm{d}k. \tag{7}$$

1.2. Eddy interaction models

We now turn our attention to the EIM. In the model, particle motions are determined by interactions with random-velocity fluid eddies. A particle remains influenced by an eddy until either the particle crosses through the eddy (when the separation between the particle and the centre of the eddy exceeds the eddy length), or the eddy dies. In the model, spatial and temporal velocity autocorrelations (and therefore wave number and frequency spectra) are characterised by the probability distributions of the eddy velocity, length and time scales.

In order to develop expressions for the energy and dissipation spectra, the analysis of Graham and James (1996) can be used. This analysis leads to expressions for the velocity autocorrelation functions $f(r)$ and $g(r)$. The analysis takes into account the fact that eddy length, lifetime, etc., can be randomly sampled (see Kallio and Reeks, 1989; Burnage and Moon, 1990; Graham, 1998a). Gosman and Ioannides' (1981) original model can be retrieved as a special case of the more general specification. This more flexible method for generating eddy characteristics still leads to a model which cannot account for the inertia effect (Wells and Stock, 1983; Reeks, 1977) or the continuity effect (Csanady, 1963) unless modified yet further. The models of Kallio and Reeks (1989) and Burnage and Moon (1990) can be considered to be *standard* in the sense that: (i) interaction times never exceed the 'eddy lifetime'; (ii) interaction times are identical in all directions.

In the standard EIM, since interaction times are identical in all directions, the longitudinal and lateral spatial correlations $f(r)$ and $g(r)$ are also identical. The energy spectrum is thus given by

$$E_{\mathrm{std}}(k) = \frac{k}{\pi}\int_0^\infty 3f(r)\sin(kr)r\,\mathrm{d}r. \tag{8}$$

In the standard EIM, $f(r)$ depends on the probability distribution of the eddy lengths (see Graham and James, 1996; Graham, 1998a):

$$f(r) = \frac{\int_r^\infty \int_l^\infty p(l')\,\mathrm{d}l'\,\mathrm{d}l}{\int_0^\infty \int_l^\infty p(l')\,\mathrm{d}l'\,\mathrm{d}l}, \tag{9}$$

where $p(l)$ is the p.d.f. of the eddy length.

In order to account for the inertia and continuity effects, Graham (1996) proposed a *modified* EIM. In particular, in order to account for the continuity effect, the EIM was modified so that interaction times in different coordinate directions could be different. In the limiting case, the interaction time in the lateral plane is exactly half that in the longitudinal direction. The modified interaction times lead to differences between longitudinal and lateral integral length scales (see Graham and James, 1996). However, these modifications to the model do not enforce incompressibility and the correlations are not related by von Karman–Howarth.

For the modified EIM, the expression for $f(r)$ is identical to that arising from the standard EIM.

$$f(r) = \frac{\int_r^\infty \int_l^\infty p(l')\,\mathrm{d}l'\,\mathrm{d}l}{\int_0^\infty \int_l^\infty p(l')\,\mathrm{d}l'\,\mathrm{d}l}. \tag{10}$$

However, the expression for g is

$$g(r) = \frac{\int_r^\infty \int_l^\infty 2p(2l')\,\mathrm{d}l'\,\mathrm{d}l}{\int_0^\infty \int_l^\infty 2p(2l')\,\mathrm{d}l'\,\mathrm{d}l}. \tag{11}$$

[N.B. The factor of 2 arising from the fact that lengths in the lateral plane are exactly half the longitudinal lengths.]

In this paper, spectral characteristics of EIMs having random-length distributions leading to polynomial or exponential spatial autocorrelation functions are investigated. For each length distribution, three different spectra are evaluated: (i) $E_{\mathrm{std}}(k)$; (ii) $E_{\mathrm{mod}}(k)$; (iii) $E_{\mathrm{vK\text{–}H}}(k)$. The first two of these of spectra arise from the standard and modified EIM, respectively. The latter arise from the same $f(r)$, but in which $g(r)$ is determined from the von Karman–Howarth relation.

The autocorrelations considered are of the form

$$f(r) = \begin{cases} \left(1 - \frac{|r|}{n+1}\right)^n & \text{if } |r| \leqslant n+1, \\ 0 & \text{otherwise,} \end{cases} \tag{12}$$

where n is an integer $\geqslant 1$. Each of these can be generated by the EIM by choosing

$$p(l') = \begin{cases} \frac{n-1}{n+1}\left(1 - \frac{l'}{n+1}\right)^{n-2} & \text{if } 0 \leqslant l' \leqslant n+1, \\ 0 & \text{otherwise,} \end{cases} \tag{13}$$

when $n > 1$. For the original EIM,

$$p(l') = \delta(l' - 2), \tag{14}$$

where $\delta(x)$ is Dirac's delta function, and the 2 appears since the eddy length must equal twice the integral length scale in this model (see Graham and James, 1996). As $n \to \infty$, the polynomial form approaches the exponential form of Kallio and Reeks (1989) and Burnage and Moon (1990):

$$p(l') = \begin{cases} e^{-l'} & \text{if } 0 \leqslant l', \\ 0 & \text{otherwise.} \end{cases} \tag{15}$$

[N.B. Other autocorrelation functions may be consistent with the EIM (see Wang and Stock, 1992, for example). However, the original EIM and the exponential model represent in a sense the two extremes available (see Graham and James, 1996 for a discussion of this point). Investigation of the polynomial correlations, which span the two extremes, should therefore give a valuable insight into the spectral properties of the EIM in general.]

For the modified EIM, we then have

$$g(r) = \begin{cases} \left(1 - \frac{2|r|}{n+1}\right)^n & \text{if } |r| \leqslant (n+1)/2, \\ 0 & \text{otherwise,} \end{cases} \tag{16}$$

which approaches

$$g(r) = e^{-2|r|} \quad \text{as } n \to \infty. \tag{17}$$

Using the von Karman–Howarth relation, on the other hand, gives

$$g(r) = \begin{cases} \left(1 - \frac{(n+2)|r|}{2(n+1)}\right)\left(1 - \frac{|r|}{n+1}\right)^{n-1} & \text{if } |r| \leqslant (n+1), \\ 0 & \text{otherwise,} \end{cases} \tag{18}$$

which approaches

$$g(r) = e^{-|r|}(1 - |r|/2) \quad \text{as } n \to \infty. \tag{19}$$

Each of these correlations is therefore related to an EIM. The remainder of this paper investigates the properties of the spectra derived from these models.

2. Evaluation of the energy and dissipation spectra

Clearly, the energy spectra will be dependent upon the value of n in the autocorrelation function. The energy spectrum for the standard EIM is given by

$$E_{\text{std}}(k) = \frac{k}{\pi} \int_0^\infty 3f(r) \sin(kr) r \, dr, \tag{20}$$

and we define

$$E_{\text{std}}(k, n) = \frac{k}{\pi} \int_0^{n+1} 3\left[1 - \frac{r}{n+1}\right]^n \sin(kr) \, dr. \tag{21}$$

For the modified EIM,

$$E_{\mathrm{mod}}(k) = \frac{k}{\pi}\int_0^\infty [f(r) + 2g(r)]\sin(kr)r\,\mathrm{d}r, \tag{22}$$

and we define

$$E_{\mathrm{mod}}(k,n) = \frac{k}{\pi}\int_0^{n+1}\left[1-\frac{r}{n+1}\right]^n r\,\mathrm{d}r + \frac{k}{\pi}\int_0^{(n+1)/2} 2\left[1-\frac{2r}{n+1}\right]^n r\,\mathrm{d}r. \tag{23}$$

When the von Karman–Howarth relation is used, the energy spectra become

$$E_{\mathrm{vK\text{–}H}}(k) = \frac{k}{\pi}\int_0^\infty [3f(r) + rf'(r)]\sin(kr)r\,\mathrm{d}r, \tag{24}$$

and we define

$$E_{\mathrm{vK\text{–}H}}(k,n) = \frac{k}{\pi}\int_0^{n+1} 3\left[1-\frac{r}{n+1}\right]^n r\,\mathrm{d}r - \frac{nk}{(n+1)\pi}\int_0^{n+1}\left[1-\frac{r}{n+1}\right]^{n-1} r^2\,\mathrm{d}r. \tag{25}$$

[N.B. This case is included for reference only – as noted above, the EIM cannot force incompressibility and the von Karman–Howarth relation does not hold for these models.]

Details of the analysis required to develop the expressions for the energy spectra are given in Appendix A. In essence, exact expressions are available for the spectra by solving certain recurrence relations. Alternatively, a computer algebra package could be used to evaluate the integrals involved. A knowledge of the form of the exact solutions enables us to make general observations about the spectra generated by *any* correlation function of the form considered here. Such details are found by careful investigation of the analytical solution.

Here, however, we concentrate on interpreting the graphical representations of these spectra. Fig. 1(a) and (b) illustrates the three energy spectra E_{std}, E_{mod} and $E_{\mathrm{vK\text{–}H}}$ for the extreme cases $n = 1$ and $n \to \infty$. Fig. 1(a) shows the spectra for the Gosman and Ioannides type model, which has delta function p.d.f.'s and linear autocorrelations (i.e. $n = 1$). In Fig 1(b), spectra are shown for the Burnage and Moon type model, which gives rise to negative-exponential correlations (i.e. $n \to \infty$). The former model is clearly prone to severe oscillation and there are indeed negative portions of the energy spectra for standard, modified and vK–H spectra. For the latter case, the magnitude of the oscillations does not decrease with increasing k. The negative portions of the energy spectrum disqualify this linear correlation from being physically reasonable. On the other hand, the energy spectra from the exponential autocorrelations are oscillation-free and strictly positive. For this model, each spectrum exhibits an 'energy-containing range' at values of k of the order of 1. There are differences in the locations and magnitudes of the peak values – these occur at $(1, 3/(2\pi))$, $(\sqrt{2}, 92/(81\pi))$ and $(\sqrt{2}, 32/(27\pi))$ for the std, mod and vK–H spectra, respectively.

It can be argued that, for a particular correlation function, the EIM is attempting to simulate the vK–H spectrum. In these terms, the std and mod spectra are roughly in phase with each other, but are out of phase with the vK–H spectrum. The importance of this decreases with increasing n (and k). For the exponential correlation, the standard EIM contains too much energy at low wave numbers and peaks too early, whereas the peak of the modified model is at the correct location, but this model contains too little energy at low wave numbers. However, for both standard and modified models, the overall shape is reasonably similar to that produced by the vK–H spectrum.

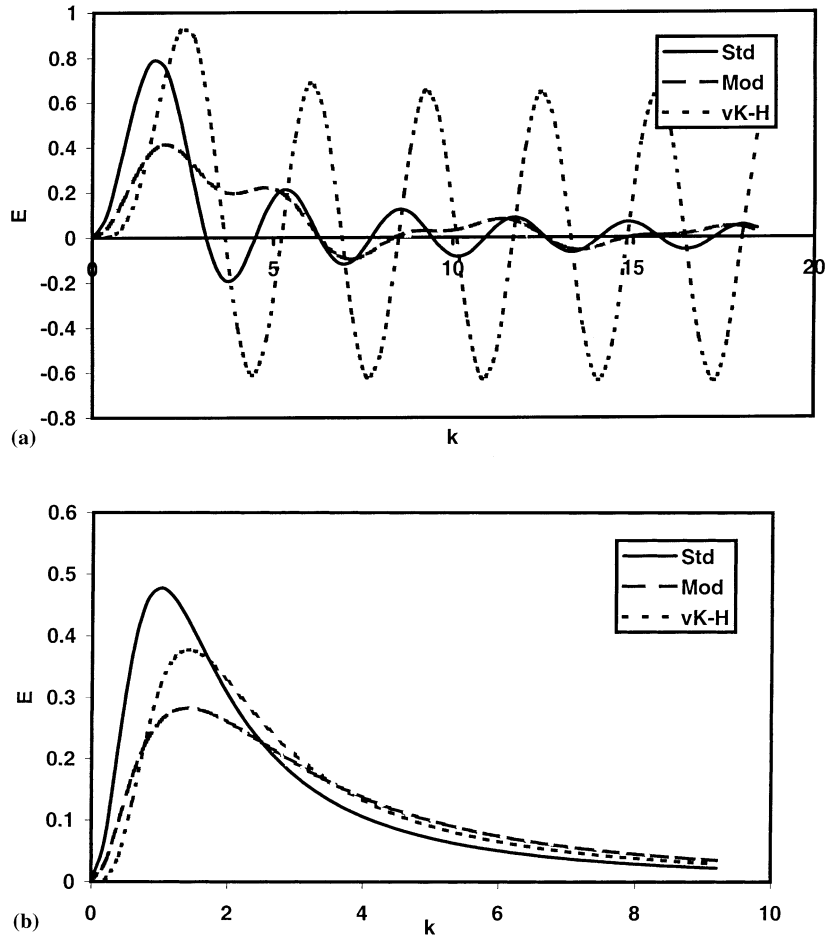

Fig. 1. Energy spectra: (a) linear correlation; (b) exponential correlation.

Figs. 2(a)–(c) illustrate the std, mod and vK–H energy spectra for $n = 2$, 4 and $n \to \infty$. The vK–H spectra are seen to be more liable to exhibit oscillatory behaviour than the other spectra. Only for $n \geqslant 3$ are the energy spectra positive definite for vK–H. Even for the vK–H spectra, however, the magnitudes of the oscillations decrease as n increases. In general, the spectra from the modified model oscillate less than those from the other two cases. In each case, the general shape converges reasonably rapidly to the $n \to \infty$ form. The change in both location and magnitude of the peak values for the std and mod spectra is significantly less than for the vK–H spectrum.

Fig. 3 gives a log–log plot of the mod energy spectrum for $n = 3$ and $n \to \infty$ and compares this with the power-law $k^{-5/3}$. In the approximate range $4 \leqslant k \leqslant 9$, the $n \to \infty$ spectrum is roughly of Kolmogorov form $\alpha k^{-5/3}$. For small k, the spectra behave like k^2, as they also do for the standard model. In contrast, the leading term for the vK–H spectra is k^4. This is explained by Batchelor (1953, p. 34) who noted the k^4 behaviour was entirely due to incompressibility and expected k^2 behaviour for compressible turbulence.

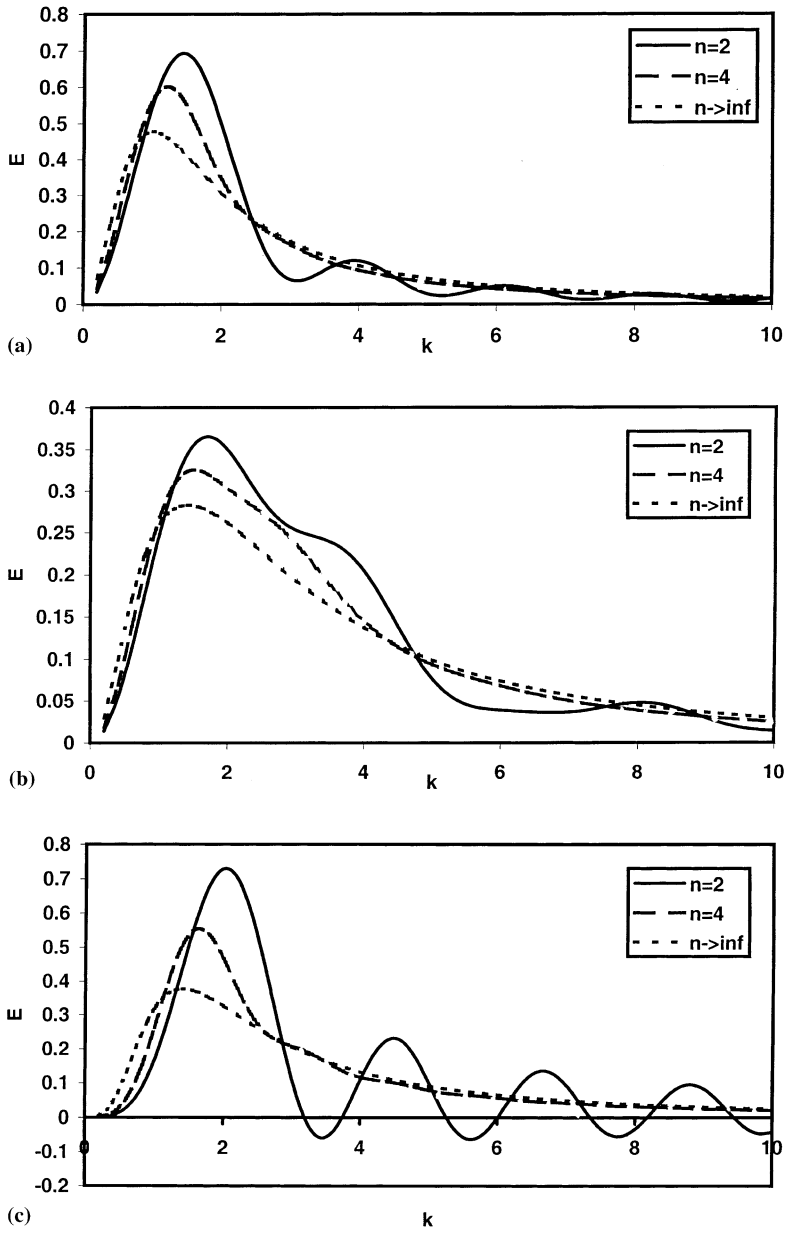

Fig. 2. Energy spectra: (a) standard; (b) modified; (c) vK–H.

At high wave numbers, the spectra are of order k^{-2}. In fact, this is true for all of the different spectral types for $n \geqslant 2$. When $n = 1$, E_{std}, E_{mod} are of order k^{-1} at higher wave numbers, whilst $E_{\text{vK–H}}$ is of order 1. This has repercussions for the dissipation spectra. The *best* of the dissipation spectra is of order 1 at high wave numbers (see Fig. 4). This means that the dissipation (Eq. (5)) from *all* of these eddy interaction models is infinite! Again, Batchelor (1953, p. 51) has an

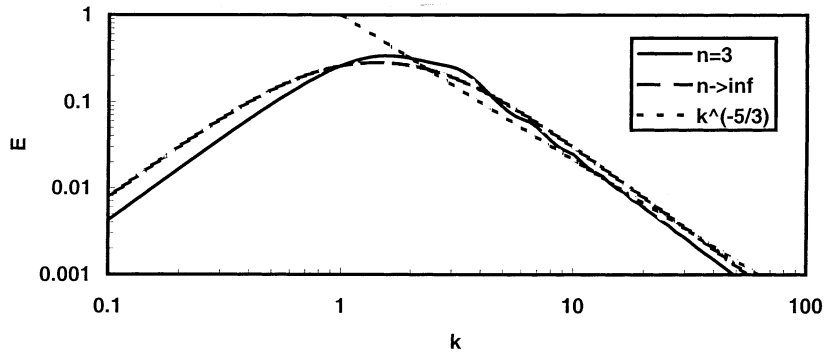

Fig. 3. Energy spectra: comparison with Kolmogorov spectrum.

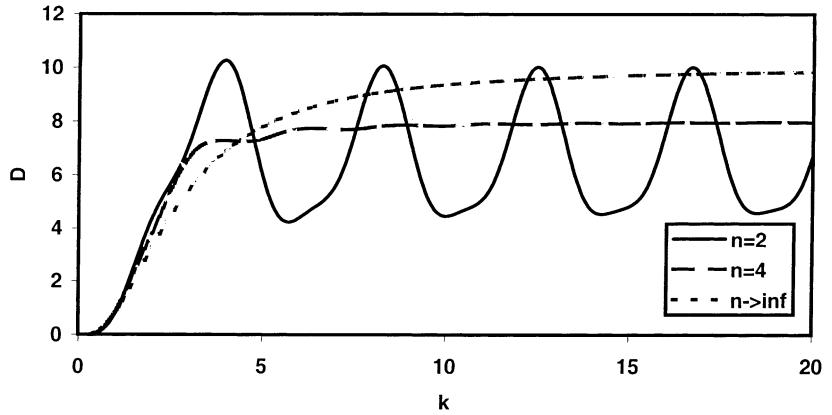

Fig. 4. Dissipation spectra: modified.

explanation. He notes that the differentials of the correlations f and g at zero separation are related to the integral moments of the energy spectrum. In particular, for incompressible turbulence,

$$-f''(0) = \frac{1}{5}\frac{\int k^2 E(k)\,\mathrm{d}k}{\int E(k)\,\mathrm{d}k}.$$

As a consequence, the dissipation is finite if and only if the second derivative $f''(0)$ exists. As noted in Graham (1997), this derivative *never* exists for the EIM. Consequently, dissipation is inevitable infinite in the EIM! [N.B. The above argument must be adapted slightly when considering the spectra from both the standard and modified EIM, since these models do not enforce incompressibility. However, similar conclusions can eventually be drawn.]

As a result of this analysis, it is possible to state that *no* EIM is capable of demonstrating completely satisfactory spectral characteristics. The spectral behaviour of the original Gosman and Ioannides (1981) model is particularly poor. In general, the characteristics improve with increasing degree n of the polynomial correlation. However, increasing n means that computation times increase. This is because the frequency of smaller eddies increases (since the mean eddy length is $(n+1)/n$) and particles will therefore cross these eddies more frequently. A reasonable

compromise, if this is problematical, is to use a polynomial correlation with $n = 2$ or 3, say. The spectrum is then reasonably smooth (particularly for the mod spectrum) and the mean length is larger than the integral scale.

It is natural to question what general conclusions on the usefulness of the EIM can be drawn from the results presented here. On the downside, we have seen that the spectra from all varieties of the model exhibit some unphysical behaviour, some cases being worse than others, and that the apparent dissipation from the models is inevitably infinite. Also, any apparent energy transfer in the model will be very different from the physical cascade from large to smaller scales (indeed, this is also true for many other Lagrangian models based upon sampling instantaneous velocities). Furthermore, the energy spectra depend on the spatial correlations, which are generally specified a priori in such models, often by specifying length scales. Clearly, there may be changes to the local turbulence energy and length scales at different points in a model-generated flow, leading to apparent changes in spectra. However, the resulting energy spectra are pre-determined in the sense that turbulence scales are determined only by local values of k or ε or both. Thus any apparent differences in spectra should not be interpreted physically. On reflection, it is clear that spectral behaviour can be inferred only from much more sophisticated (and expensive) DNS models.

The spectral analysis has shown that EIM models are relatively unsuccessful at predicting small-scale behaviour. This is the case even if the models are modified to take into account the CTE, inertia and continuity effects. One cause must be that, whilst the true motions at these scales are constrained by viscous dissipation, the motions in the models are unaffected by viscosity. Another is that they do not enforce incompressibility, so that motions in different coordinate directions are not sufficiently cross-correlated. Similar conclusions can be drawn for many related Lagrangian models. More sophisticated models such as DNS must be used in order for these influences to be accommodated.

On the positive side, the EIM and similar models are mainly used to predict the dispersion of solid particles in turbulent flows. This dispersion is controlled by the large-scale fluid motions. The ability of the models to cater for these large-scale motions remains undiminished. Thus, for example, the modified EIM successfully models the CTE, inertia and continuity effects. In more complex flows, the performance of the models is influenced by the lack of detailed measurements of the associated large length and time scales. It is reasonably straightforward to force the models to use the correct integral length and time scales if the scales are known. The fact that these scales are generally unknown experimentally is, however, a major problem in such modelling! At present, rather coarse approximations must be used. Nevertheless, the models can still be used successfully to produce useful information on phenomena such as dispersion and deposition, even in the most complex flows. The unrealistic behaviour of the small-scale regions of the energy spectra is relatively unimportant in such situations.

3. Conclusions

Energy and dissipation spectra arising from EIMs have been evaluated. The energy spectra are determined by the Eulerian longitudinal and lateral spatial correlations $f(r)$ and $g(r)$, respectively. Polynomial expressions for the correlations have been considered. Such polynomial correlations

can be produced using random eddy lengths in the EIM. Spectra for both the standard EIM (i.e. the Gosman and Ioannides (1981), model, which allows for the CTE but not the inertia and continuity effects) and Graham (1996), modified EIM (which allows for all three effects) have been derived. In addition, the spectra produced using the von Karman–Howarth relation are given. The following conclusions can be drawn:

1. there are negative portions, and oscillations, of the energy spectrum for small values of n, which disappear for larger n;
2. as $n \to \infty$, the location of the peak of the energy spectrum is similar for the modified EIM and the von Karman–Howarth case;
3. for large n, there is an approximate Kolmogorov range where $E(k)$ is roughly proportional to $k^{-5/3}$;
4. as $k \to \infty$, the spectra are at best $o(k^{-2})$, implying that the dissipation ε is infinite for these models;
5. whilst the models are less successful at predicting small-scale motions, the ability of the models to reflect the large-scale motions that influence turbulent dispersion is undiminished.

Appendix A

We are interested in integrals of the form:

$$A_m^\alpha = \int_0^\alpha r\left[1-\frac{r}{\alpha}\right]^m \sin(kr)\,\mathrm{d}r \tag{A.1}$$

and

$$B_m^\alpha = \int_0^\alpha r^2\left[1-\frac{r}{\alpha}\right]^m \sin(kr)\,\mathrm{d}r. \tag{A.2}$$

Now

$$\begin{aligned} A_m^\alpha &= \alpha\int_0^\alpha \left[1-\frac{r}{\alpha}\right]^m \sin(kr)\,\mathrm{d}r - \alpha\int_0^\alpha \left[1-\frac{r}{\alpha}\right]^{m+1} \sin(kr)\,\mathrm{d}r \\ &= \alpha\left[I_m^\alpha - I_{m+1}^\alpha\right] \end{aligned} \tag{A.3}$$

and

$$\begin{aligned} B_m^\alpha &= \int_0^\alpha \left[\alpha^2\left(1-\frac{r}{\alpha}\right)^{m+2} + \alpha[2r-\alpha]\left(1-\frac{r}{\alpha}\right)^m\right]\sin(kr)\,\mathrm{d}r, \\ &= \alpha^2 I_{m+2}^\alpha + 2\alpha^2\left[-I_{m+1}^\alpha + I_m^\alpha\right] - \alpha^2 I_m^\alpha, \\ &= \alpha^2\left[I_{m+2}^\alpha - 2I_{m+1}^\alpha + I_m^\alpha\right], \end{aligned} \tag{A.4}$$

where

$$I_m^\alpha = \int_0^\alpha \left[1-\frac{r}{\alpha}\right]^m \sin(kr)\,\mathrm{d}r. \tag{A.5}$$

The energy spectra are then given by

$$E_{\text{std}} = 3A_n^{n+1},$$
$$E_{\text{mod}} = A_n^{n+1} + A_n^{(n+1)/2}, \tag{A.6}$$
$$E_{\text{vK–H}} = 3A_n^{n+1} - \frac{n}{n+1} B_{n-1}^{n+1}.$$

Thus all of these spectra can be expressed in terms of the integrals I_m^α. We next find a recurrence relation to determine these integrals. Integrating by parts gives

$$I_m^\alpha = \frac{1}{k} - \frac{m(m-1)}{k^2\alpha^2} I_{m-2}^\alpha. \tag{A.7}$$

This relation, along with the integrals

$$I_0^\alpha = \frac{1}{k}[1 - \cos(k\alpha)] \tag{A.8}$$

and

$$I_1^\alpha = \frac{1}{k}\left[1 - \frac{1}{k}\sin(k\alpha)\right] \tag{A.9}$$

enables any of the I_m^α to be evaluated.

The solution is as follows.For even m,

$$I_m^\alpha = \frac{1}{k} + \frac{1}{k}\sum_{l=1}^{m/2-1} \frac{m!}{(2l)!}\left[\frac{-1}{k^2\alpha^2}\right]^{m/2-l} + \frac{(-1)^{(m/2)} m! I_0^\alpha}{k^m \alpha^m}, \tag{A.10}$$

whereas, for odd m,

$$I_m^\alpha = \frac{1}{k} + \frac{1}{k}\sum_{l=1}^{(m-1)/2-1} \frac{m!}{(2l+1)!}\left[\frac{-1}{k^2\alpha^2}\right]^{(m-1)/2-l} + \frac{(-1)^{(m-1)/2} m! I_1^\alpha}{k^{m-1}\alpha^{m-1}}. \tag{A.11}$$

References

Batchelor, G.K., 1953. Homogeneous Turbulence. Cambridge University Press, Cambridge.

Boivin, M., Simonin, O., Squires, K.D., 1999. Direct numerical simulation of turbulence modulation by particles in isotropic turbulence. J. Fluid Mech. 375, 235–263.

Burnage, H., Moon, S., 1990. Prediction of the dispersion of material particles in a turbulent flow. C.R. Acad Sci. Paris, t310, Serie II, pp. 1595–1600.

Csanady, G.T., 1963. Turbulent diffusion of heavy particles in the atmosphere. J. Atmos. Sci. 20, 201–208.

Elghobashi, S.E., Truesdell, G.C., 1993. On the two-way interaction between homogeneous turbulence and dispersed particles. I: Turbulence modification. Phys. Fluids A 5, 1790–1801.

Gosman, A.D., Ioannides, E., 1981. Aspects of Computer Simulation of Liquid Fuelled Combustors. Paper AIAA-81-0323, AIAA 19th Aerospace Sciences Mtg., St. Louis, USA.

Graham, D.I., 1996. An improved eddy interaction model for prediction of turbulent particles dispersion. ASME J. Fluids Eng. 118, 819–823.

Graham, D.I., 1997. Turbulence modulation in eddy interaction models. In: Symposium on Gas/Particle Flows, ASME FED Summer Meeting, Vancouver, BC, Canada.

Graham, D.I., 1998a. Improved eddy interaction models with random length and time scales. Int. J. Multiphase Flow 24, 335–345.

Graham, D.I., 1998b. Analytical comparison of Lagrangian particle dispersion models. Paper number 125, ICMF'98, Lyon, France.

Graham, D.I., James, P.W., 1996. Turbulent dispersion using eddy interaction models. Int. J. Multiphase Flow 22, 57–75.

Hetsroni, G., 1989. Particles–turbulence interaction. Int. J. Multiphase Flow 15, 735–746.

Hussainov, M., Kartushinsky, A., Rudi, U., Shcheglov, I., Kohnen, G., Sommerfeld, M., 1999. Modification of grid-generated turbulence in air–dust flow. Paper FEDSM99-7878. In: Symposium on Gas/Particle Flows, ASME FED Summer Meeting, San Francisco, CA, USA.

Kallio, G., Reeks, M.W., 1989. A numerical simulation of particle deposition in turbulent boundary layers. Int. J. Multiphase Flow 15, 433–446.

Lance, M., Bataille, J., 1991. Turbulence in the liquid phase of a uniform bubbly air–water flow. J. Fluid Mech. 222, 95–118.

Reeks, M.W., 1977. On the dispersion of small particles suspended in an isotropic turbulent fluid. J. Fluid Mech. 83, 529–546.

Schreck, S., Kleis, S.J., 1993. Modification of grid-generated turbulence by solid particles. J. Fluid Mech. 249, 665–688.

Snyder, W.H., Lumley, J.L., 1971. Some measurements of particle velocity autocorrelation functions in turbulent flow. J. Fluid Mech. 48, 41–71.

Squires, K.D., Eaton, J.K., 1990. Particle response and turbulence modification in isotropic turbulence. Phys. Fluids A 2, 1191–1203.

Squires, K.D., Eaton, J.K., 1991. Lagrangian and Eulerian statistics obtained from direct numerical simulations of homogeneous turbulence. Phys. Fluids A 3, 130–143.

Sundaram, S., Collins, L.R., 1999. A numerical study of the modulation of isotropic turbulence by suspended particles. J. Fluid Mech. 379, 105–143.

Tennekes, H., Lumley, J.L., 1972. A First Course in Turbulence. MIT Press, Cambridge, MA.

Wang, L.-P., Stock, D.E., 1992. Stochastic trajectory models for turbulent diffusion: monte carlo process versus markov chains. Atm. Envir. A 26, 1599–1607.

Wells, Stock, D.E., 1983. The effects of crossing trajectories on the dispersion of particles in a turbulent flow. J. Fluid Mech. 136, 31–62.